

# Position of Propellant in Teardrop Tank Systems

Masahiko Utsumi\*

*Ishikawajima-Harima Heavy Industries Company, Ltd., Tokyo 135, Japan*

The position of liquid propellant in a teardrop tank system is determined to estimate the propellant mass distributions of the tanks, the center of gravity, and the inertia tensors of the satellite-liquid system. The fairly large displacement of the center of spin caused by the detachment of objects from the satellite is discussed. A double-loop iteration algorithm is applied to determine the center of spin inasmuch as it cannot be prescribed. Numerical computation for symmetric and asymmetric cases reveals a considerably large critical value of the total propellant mass at which some of the tanks empty and a large tilt of the principal inertia axis occurs. It is pointed out that, so as to not underrate the tilt of the principal inertia axis, one should not approximate the tank shape as a sphere but perform the integration over the liquid volume exactly, although it is geometrically complicated, i.e., the domain surrounded by conical and spherical tank walls and parabolic liquid surface.

## Nomenclature

$a$	= radius of spherical part of tanks (Fig. 1), m
$b$	= $a/\sin \theta_c$ (Fig. 1), m
$d_i$	= distance between $z$ axis and center of spherical part of tank $i$ (Fig. 1), m
$G$	= center of gravity of satellite-liquid system
$g$	= gravity acceleration due to vehicle propulsion, $m/s^2$
$H$	= distance between $x_i$ axis and top of conical part of tank (Fig. 1), m
$i$	= tank number
$L$	= distance between $z$ axis and top of conical part of tank (Fig. 1), m
$M_f$	= total propellant mass in tank system, kg
$M_{fcr}$	= critical total propellant mass, kg
$M_{fi}$	= propellant mass in tank $i$ , kg
$p$	= pressure of liquid propellant, $N/m^2$
$(R_i, \theta_i, \varphi_i)$	= spherical coordinates for tank $i$
$(x, y, z)$	= coordinates fixed to spinning satellite (Fig. 1), m
$(x_{fGi}, y_{fGi}, z_{fGi})$	= $(x, y, z)$ coordinates of center of gravity of propellant in tank $i$ , m
$(x_G, y_G, z_G)$	= $(x, y, z)$ coordinates of $G$ , m
$(x_i, y_i, z_i)$	= coordinates for tank $i$ (Fig. 1), m
$(\tilde{x}_i, \tilde{y}_i, \tilde{z}_i)$	= geometrical centerline of tank system (Fig. 1)
$z$	= circumferential coordinate of tank $i$ measured from $x$ axis (Fig. 1)
$\alpha_i$	= angle between tank axis $\tilde{z}_i$ and $z$ axis (Fig. 1)
$\gamma$	= half the apex angle of conical part of the tanks (Fig. 1)
$\theta_c$	= tilt of principal inertia axis of satellite-liquid system against $\zeta$ axis
$\theta_{tilt}$	= coordinates fixed to the spinning satellite (Fig. 1), m
$(\xi, \eta, \zeta)$	= density of liquid propellant, $kg/m^3$
$\rho$	= angular velocity of spin, $rad/s$
$\Omega$	

## Subscripts

$f$	= fluid (liquid propellant)
$i$	= tank number

$r$	= rigid body (main body of satellite and objects to be detached)
-----	--

## Introduction

**S**TABILIZATION of an artificial satellite is accomplished by spinning. For the spinning satellite, the propellant is supplied by a teardrop tank system. The geometry of such a tank system is shown in Fig. 1, where the teardrop-shaped form of the tanks is given by spherical and conical surfaces and arranged in circumferential 120-deg pitch with one generatrix of the conical surfaces nearly parallel to the spin axis  $z$ . The purpose of the teardrop tank system is to hold liquid propellant at the outlet of each tank (the top of the conical surface) by utilizing centrifugal force due to spinning and gravity force  $g$  caused by the acceleration of the vehicle propulsion. That is, by dint of the presence of the conical part in each tank, the propellant can be held at the outlet of each tank irrespective of the relative magnitude of the centrifugal force and the gravity force  $g$ .

The purpose here is to determine the stationary position of the liquid propellant for the case where the center of gravity is displaced largely from its original favorable position on the  $z$  axis, i.e., the geometric centerline of the tank system without liquid. This occurs when some objects of not negligibly small mass compared with the main body are detached from the satellite. An important example is the satellite LUNAR-A, whose mission is to detach three objects every few weeks and send them to the moon for examination of physical conditions at various places on the lunar surface.<sup>1</sup>

Quantities of concern are 1) the propellant mass distribution over the three tanks and 2) the position of the center of gravity and inertia tensors of the satellite-liquid system. The former is essential for evaluating the efficiency of the propellant consumption, whereas the latter are necessary parameters for detailed dynamics and control analysis of the satellite.

Some papers exist concerned with the determination of the liquid position in a teardrop tank system<sup>2,3</sup> and a tank with a propellant management device.<sup>4-7</sup> However, thus far no investigation has been made of objects relatively massive compared with the main body mass of the satellite or of a displacement of the center of gravity from its original favorable position so large that some of the tanks empty. Considering both aspects is one of the original points of the present paper.

Another feature of this paper is that the mass, position of the center of gravity, and inertia tensors of the liquid in each tank are calculated precisely by accurate volume integration over the liquid domain surrounded by the conical and spherical tank walls and the parabolic liquid surface (see Fig. 1). Conventional studies approximate the teardrop tank as a spherical tank by neglecting the conical part of the teardrop shape.<sup>2,3</sup> In addition, the curved liquid surface in each tank is approximated by a plane. This approximation is not valid, in particular, when the tank system is confined in a satellite compactly and the tanks are close to each other, as they are in the

Received Nov. 18, 1996; revision received June 30, 1997; accepted for publication July 12, 1997. Copyright © 1997 by the American Institute of Aeronautics and Astronautics, Inc. All rights reserved.

\*Section Manager, Machine Element Department, Research Institute, 3-1-15, Toyosu, Koto-ku.

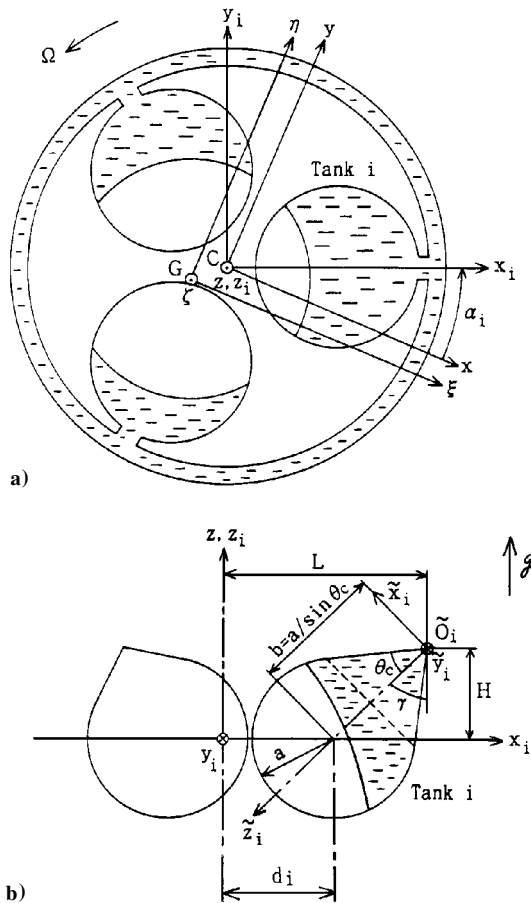


Fig. 1 Teardrop tank system and coordinate systems;  $\tilde{O}_i$  is outlet for propellant in tank  $i$ .

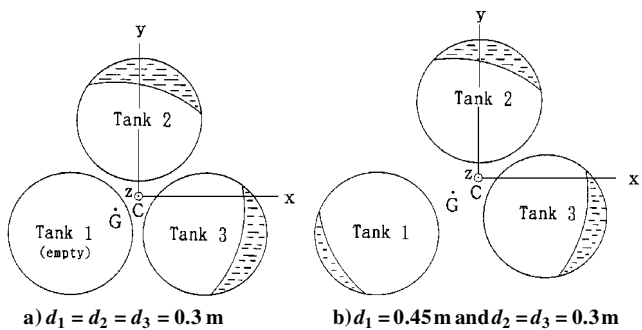


Fig. 2 Propellant distribution when object 1 is detached (total propellant mass  $M_f = 20$  kg).

practical example here (Figs. 1 and 2). Hence, a precise calculation is necessary.

It is shown by numerical results that the detachment of objects from the satellite gives rise to serious problems in the engine propulsion system as well as the attitude control system. Subsequently, a method for solving the problems is developed, and its validity is ascertained by the numerical calculations.

Teardrop Tank System and Coordinate Systems

If there is no eccentricity in Fig. 1, the system spins around the  $z$  axis, the geometrical centerline of the tank system without liquid propellant, and the propellant is distributed equally over the three tanks. However, when rotational imbalance is caused by the detachment of objects from the satellite, the center of gravity of the system, represented by  $G$  in Fig. 1, moves from its original position on the  $z$  axis so that the system spins around another axis, e.g., the  $\zeta$  axis

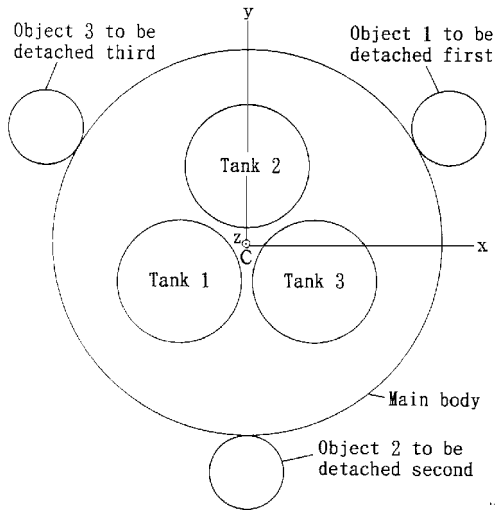


Fig. 3 Numerical example.

shown in Fig. 1, which passes through  $G$ . As a result of this, the liquid propellant masses  $M_{fi}$  of the three tanks are not equal to each other. That is, the displacement of the center of gravity gives rise to propellant migration among the tanks. In the eccentric case, the centerline  $z$  axis is no longer an actual spin axis but only a nominal axis.

The purpose is to determine the stationary position of the propellant for the eccentric case. The position will be determined by the equilibrium condition among the centrifugal forces due to the angular spinning velocity  $\Omega$ , the gravity force due to the acceleration of the vehicle propulsion  $g$ , and the gas pressure in each tank. The gas pressure supplied to each tank is assumed to be common because the gas in each tank is connected by pipes (not shown in Fig. 1 to keep the figure uncomplicated).

Practical examples of the imbalance will be given in the section that is dedicated to the description of the numerical model (Fig. 3). This paper considers the case where the  $z$  coordinates of the centers of gravity of all of the components of the system, i.e., the main body of the satellite without propellant, the objects to be detached, and the propellant, are close to 0. Thus, the  $z$  component of the displacement vector of the center of gravity  $G$  from its original position is small. Such a case is common and favorable for the sake of weight balancing and allows us to make the approximation that the  $z$  axis is parallel to the  $\zeta$  axis.

Note that, for the problem under consideration, the position of the center of gravity  $G$  is unknown or cannot be prescribed because  $G$  is the center of gravity of the whole satellite-liquid system and the liquid position within the system depends on the center of spinning, which coincides with  $G$ . That is, if we determine the liquid position under the assumed position of the center of spinning  $G_{old}$  and calculate the center of gravity  $G_{new}$  of the satellite-liquidsystem,  $G_{new}$  does not necessarily coincide with  $G_{old}$ . Therefore, for the determination of the position of  $G$ , we must resort to iterative procedures, where the calculation of  $G_{new}$  under the assumed  $G_{old}$  is repeated such that  $G_{new}$  coincides with  $G_{old}$ . Iterative procedures are also required for determining the position of the liquid surface for the prescribed total propellant mass in the tank system, so that double-loop iteration procedures are needed. Through these procedures, we can determine the liquid mass in each tank, as well as the position of the center of gravity and the inertia tensors of the whole satellite-liquid system.

Coordinate systems used for the subsequent analysis are shown in Fig. 1. These are defined as follows. First,  $G-\xi\eta\zeta$  and  $C-xyz$  are the rotating coordinate systems fixed to the spinning satellite. The relation between them is

$$\begin{Bmatrix} \xi \\ \eta \\ \zeta \end{Bmatrix} = \begin{Bmatrix} x - x_G \\ y - y_G \\ z - z_G \end{Bmatrix} \tag{1}$$

Second, define the coordinate system  $C-x_i y_i z_i$  for each tank  $i$  ( $i = 1-3$ ) by rotating  $C-xyz$  the angle  $\alpha_i$  around the  $z$  axis (see Fig. 1a):

$$\begin{Bmatrix} x \\ y \\ z \end{Bmatrix} = \begin{bmatrix} \cos \alpha_i & -\sin \alpha_i & 0 \\ \sin \alpha_i & \cos \alpha_i & 0 \\ 0 & 0 & 1 \end{bmatrix} \begin{Bmatrix} x_i \\ y_i \\ z_i \end{Bmatrix} \quad (2)$$

where  $\alpha_i$  represents the circumferential coordinate of  $\tilde{O}_i$  (the propellant outlet of tank  $i$ ) measured from the  $x$  axis.

Third, set the coordinate system  $\tilde{O}_i-\tilde{x}_i \tilde{y}_i \tilde{z}_i$  for the tank  $i$  ( $i = 1-3$ ) by rotating  $C-x_i y_i z_i$  the angle  $\pi - \gamma$  around the  $y_i$  axis and shifting the origin  $C$  by length  $L$  in the  $x_i$  direction and height  $H$  in the  $z_i$  direction:

$$\begin{Bmatrix} x_i \\ y_i \\ z_i \end{Bmatrix} = \begin{bmatrix} -\cos \gamma & 0 & -\sin \gamma \\ 0 & 1 & 0 \\ \sin \gamma & 0 & -\cos \gamma \end{bmatrix} \begin{Bmatrix} \tilde{x}_i \\ \tilde{y}_i \\ \tilde{z}_i \end{Bmatrix} + \begin{Bmatrix} L \\ 0 \\ H \end{Bmatrix} \quad (3)$$

### Stationary Position of Liquid Propellant

#### Equation for the Liquid Surfaces

Because the problem under consideration is to determine the stationary position of the propellant, basic equations can be derived from the Navier-Stokes equation by neglecting the fluid velocity components, i.e.,

$$\Omega^2 \xi - \frac{1}{\rho} \frac{\partial p}{\partial \xi} = 0 \quad (4a)$$

$$\Omega^2 \eta - \frac{1}{\rho} \frac{\partial p}{\partial \eta} = 0 \quad (4b)$$

$$g - \frac{1}{\rho} \frac{\partial p}{\partial \zeta} = 0 \quad (4c)$$

where Eqs. (4a) and (4b) correspond to the equilibrium condition between the pressure gradient and the centrifugal force, whereas Eq. (4c) corresponds to the equilibrium between the pressure gradient and the gravity force. Integrating Eqs. (4a-4c), one obtains

$$p = C_1 + \rho g \zeta + \frac{1}{2} \rho \Omega^2 (\xi^2 + \eta^2) \quad (5)$$

where  $C_1$  is an arbitrary constant. By using the condition that the gas pressure supplied to all of the tanks is  $p_g$ , the liquid surface shape  $\zeta = \zeta_{st}(\xi, \eta)$  can be determined as

$$\zeta_{st}(\xi, \eta) = \frac{p_g - C_1}{\rho g} - \frac{\Omega^2}{2g} (\xi^2 + \eta^2) \quad (6)$$

which means that the liquid surface is a parabolic surface whose axis is the  $\zeta$  axis. When the centrifugal force is predominant to the gravity force, the liquid surface tends to a cylindrical surface. The arbitrary constant  $C_1$  in Eq. (6) can be determined by the condition that the total liquid mass contained in tanks 1-3 equals a certain prescribed value.

#### Mass, Center of Gravity, and Inertia Tensors of the Liquid

For a precise estimation of the mass distribution, the center of gravity, and inertia tensors of the liquid propellant, it is necessary to perform a volume integration over the liquid domain, as pointed out in the Introduction. For the volume integration, a spherical coordinate system  $(R_i, \theta_i, \varphi_i)$  is used, whose origin is at the intersection of the spherical surface of tank  $i$  and the tank axis  $\tilde{z}_i$ . The axis of the spherical coordinate system is the  $\tilde{z}_i$  axis. Therefore, the relation between the coordinate systems  $(R_i, \theta_i, \varphi_i)$  and  $(\tilde{x}_i, \tilde{y}_i, \tilde{z}_i)$  is

$$\tilde{x}_i = R_i \sin \theta_i \cos \varphi_i, \quad \tilde{y}_i = R_i \sin \theta_i \sin \varphi_i \quad (7)$$

$$\tilde{z}_i = a + b - R_i \cos \theta_i$$

The relation between  $(R_i, \theta_i, \varphi_i)$  and  $(\xi, \eta, \zeta)$  can be derived for  $i = 1, 2$ , and 3 in the form

$$\xi_k = C_{ik1} R_i + C_{ik0} \quad (8)$$

by using Eqs. (1-3) and (7). In Eq. (8),  $\xi_1, \xi_2$ , and  $\xi_3$  represent  $\xi, \eta$ , and  $\zeta$ , respectively, and  $C_{ik1}$  and  $C_{ik0}$  can be expressed as functions of  $\theta_i$  and  $\varphi_i$ . By using spherical coordinates, the mass  $M_{fi}$ ,  $(x, y, z)$  coordinates of the center of gravity, and the inertia tensor matrix  $I_{fi}$  of the liquid in each tank  $i$  can be calculated, respectively, by

$$M_{fi} = \rho \int_0^{2\pi} \int_0^{\tilde{\theta}_i} \int_{R_{iM}}^{R_{iW}} R_i^2 \sin \theta_i dR_i d\theta_i d\varphi_i \quad (9)$$

$$\begin{Bmatrix} x_{fGi} \\ y_{fGi} \\ z_{fGi} \end{Bmatrix} = \rho \int_0^{2\pi} \int_0^{\tilde{\theta}_i} \int_{R_{iM}}^{R_{iW}} \begin{Bmatrix} \xi + x_G \\ \eta + y_G \\ \zeta + z_G \end{Bmatrix} R_i^2 \sin \theta_i dR_i d\theta_i \frac{d\varphi_i}{M_{fi}} \quad (10)$$

and

$$I_{fi} = \begin{bmatrix} S_{i22} + S_{i33} & -S_{i12} & -S_{i13} \\ S_{i33} + S_{i11} & -S_{i23} & \\ \text{sym} & & S_{i11} + S_{i22} \end{bmatrix} \quad (11)$$

where

$$S_{ikl} = \rho \int_0^{2\pi} \int_0^{\tilde{\theta}_i} \int_{R_{iM}}^{R_{iW}} \xi_k \xi_l R_i^2 \sin \theta_i dR_i d\theta_i d\varphi_i \quad (12)$$

In the volume integrations of Eqs. (9), (10), and (12),  $R_{iM}$  and  $R_{iW}$  are the  $R_i$  coordinates of the liquid surface and the tank wall, respectively, whereas  $\tilde{\theta}_i$  is the  $\theta_i$  coordinate of the contact line of the liquid surface with the tank wall. Evaluation of the actual form of the functions  $\tilde{\theta}_i(\varphi_i)$ ,  $R_{iM}(\theta_i, \varphi_i)$ , and  $R_{iW}(\theta_i, \varphi_i)$  is straightforward and is outlined in the Appendix.

### Numerical Results

#### Numerical Example

The numerical calculation is performed for the following case:  $\rho = 1009 \text{ kg/m}^3$ ,  $\Omega = 4\pi \text{ rad/s}$  (120 rpm),  $g = 0.5 \text{ m/s}^2$ ,  $a = 0.24 \text{ m}$ ,  $\theta_C = 40 \text{ deg}$ ,  $\gamma = 42 \text{ deg}$ ,  $\alpha_1 = 210 \text{ deg}$ ,  $\alpha_2 = 90 \text{ deg}$ ,  $\alpha_3 = -30 \text{ deg}$  (see Fig. 3),  $L = 0.550 \text{ m}$ , and  $H = 0.278 \text{ m}$ . In this case, the center of the spherical surface of tank  $i$  is 0.3 m away from the  $z$  axis and lies in the plane  $z = 0$ . The gravity  $g$  is chosen to be an arbitrary value for which the liquid surface becomes cylindrical. This corresponds to the part of mission just before the detachment.

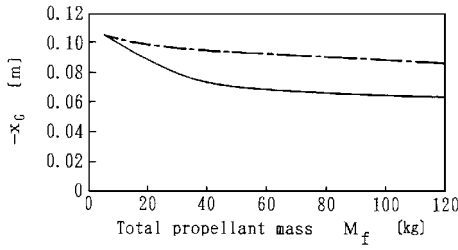
The mass and the inertia tensors of the main body of the satellite without liquid propellant are, respectively,  $M_{ro} = 200 \text{ kg}$ ,  $I_{roxx} = I_{royy} = 60 \text{ kgm}^2$ ,  $I_{roz z} = 80 \text{ kgm}^2$ , and  $I_{roxy} = I_{royz} = I_{roz x} = 0$ . The center of gravity is at  $x = y = z = 0$ .

The common mass of the objects  $j$  that are to be detached ( $j = 1-3$ ; see Fig. 3) is  $M_{rj} = 40 \text{ kg}$ . As shown in Fig. 3, the centers of gravity of objects 1, 2, and 3 are located at the opposite side of the  $z$  axis from the tanks 1, 2, and 3, respectively, i.e., at 30, -90, and 150 deg in the circumferential direction measured from the  $x$  axis. All three of these centers of gravity are on the circle  $\sqrt{(x^2 + y^2)} = 0.9 \text{ m}$  in the plane  $z = 0$ . The common inertia tensors of each object  $j$  ( $j = 1, 2$ , and 3) around its principal inertia axes  $\alpha$ ,  $\beta$ , and  $\gamma$  are  $I_{rj\alpha\alpha} = I_{rj\beta\beta} = 4 \text{ kgm}^2$ ,  $I_{rj\gamma\gamma} = 0.4 \text{ kgm}^2$ , and  $I_{rj\alpha\beta} = I_{rj\beta\gamma} = I_{rj\gamma\alpha} = 0$ , where the  $\alpha$ ,  $\beta$ , and  $\gamma$  axes are parallel to the  $x$ ,  $y$ , and  $z$  axes, respectively, and pass through the center of gravity of each object  $j$ .

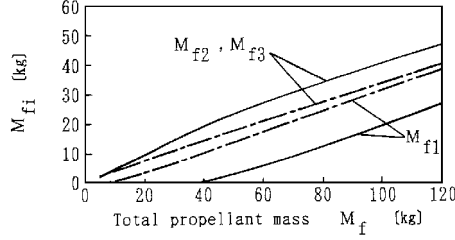
#### Satellite-Liquid System with Object 1 Detached

First, the numerical calculation is performed for the case where object 1 is detached and objects 2 and 3 are retained. The results for this case are illustrated by the solid lines in Fig. 4 showing the coordinate  $x_G$  of the center of gravity for the whole satellite-liquid system (Fig. 4a), the propellant masses  $M_{fi}$  in each tank  $i$  ( $i = 1-3$ ) (Fig. 4b), the tilt  $\theta_{ilt}$  of the principal inertia axis against the  $\zeta$  axis (Fig. 4c), and the coordinate  $z_{fGi}$  of the centers of gravity for the liquid propellant in each tank  $i$  (Fig. 4d) as functions of the total propellant mass

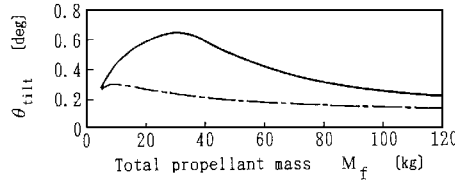
$$M_f = \sum_{i=1}^3 M_{fi}$$



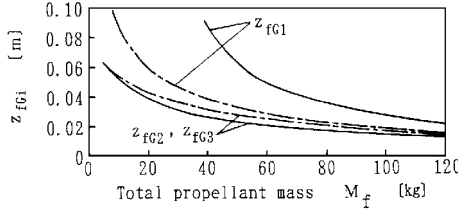
a)  $x$  coordinate  $x_G$  of the center of gravity for whole satellite-liquid system



b) Propellant masses  $M_{fi}$  in the tanks  $i$  ( $i = 1, 2, 3$ )



c) Tilt  $\theta_{\text{tilt}}$  of principal inertia axis vs  $\zeta$  axis



d)  $z$  coordinate  $z_{fGi}$  of the centers of gravity for liquid propellant in the tanks  $i$  ( $i = 1, 2, 3$ )

**Fig. 4** Numerical results for the case where object 1 is detached: —,  $d_1 = d_2 = d_3 = 0.3$  m and ---,  $d_1 = 0.45$  m;  $d_2 = d_3 = 0.3$  m.

Figure 2a shows a typical example of the propellant distribution in each tank for the case  $M_f = 20$  kg. In the numerical example, the centrifugal force is predominant in comparison with the gravity, so that the parabolic liquid surface in each tank is almost cylindrical, as shown by Fig. 2a. Moreover, the following two points are noted due to the symmetry of the problem about the plane  $y = x/\sqrt{3}$ .

1) The value of  $y_G$  is easily found by multiplying  $x_G$ , which is shown in Fig. 4a, by  $1/\sqrt{3}$ .

2) As shown by Fig. 4b,  $M_{f2} = M_{f3}$  is satisfied. That is, the propellant masses in tanks 2 and 3 are equal to each other.

It can be seen from Figs. 2a and 4a that the displacement of  $G$  from its original position, i.e., the  $z$  axis, is not negligibly small compared to the tank size. This results in such a large imbalance between  $M_{f1}$  and  $M_{f2} (= M_{f3})$  that tank 1, which is nearest to  $G$ , empties ( $M_{f1} = 0$ ) when the total propellant mass  $M_f$  is smaller than the fairly large critical value  $M_{fcr} = 37$  kg (cf. lower solid line in Fig. 4b). Figure 2a corresponds to the case  $M_f = 20$  kg, which is much smaller than the critical value  $M_{fcr} = 37$  kg. When the total propellant mass is smaller than the critical value, the relation  $M_{f2} = M_{f3} = 0.5M_f$  is satisfied, as shown in Fig. 4b.

Figure 4a shows that to a certain extent the migration of the liquid propellant restores the center of gravity  $G$  to its original position. This can be understood by considering the extreme case  $M_f = 0$ , i.e., the case in which the system has no liquid at all. In this case, the detachment of object 1 moves the center of gravity of the system from  $x = 0$  to  $x = -0.111$  m, which can be found as the limit of

$x_G$  when  $M_f \rightarrow 0$  (see Fig. 4a). One can find from Fig. 4a that the center of gravity for nonzero  $M_f$  is always closer to the  $z$  axis than that for  $M_f = 0$ . The larger  $M_f$  is, the closer  $G$  gets to the  $z$  axis. Thus, the migration of the liquid propellant among the tanks has an effect of restoring the center of gravity  $G$  to its original position to some degree.

It is interesting that in Fig. 4a  $dx_G/dM_f$  clearly changes near the critical value of the total propellant mass  $M_{fcr} = 37$  kg, under which tank 1 is empty. The value of  $|dx_G/dM_f|$  is larger in the range  $0 < M_f < M_{fcr}$  than in the range  $M_{fcr} < M_f$ . That is, the increasing rate of restoring the center of gravity with the augmentation of  $M_f$  is more remarkable when tank 1 is empty than when no tank is empty.

Figure 4c shows the tilt  $\theta_{\text{tilt}}$  of the principal inertia axis vs the  $\zeta$  axis. This can be calculated by the eigenvectors of the inertia tensor matrix of the whole satellite-liquid system. Figure 4c shows the following important result. Although the tilt is caused by the presence of the propellant,  $\theta_{\text{tilt}}$  does not necessarily decrease monotonically with the decrease of the total propellant mass  $M_f$  but exhibits a maximum near the critical total propellant mass  $M_{fcr} = 37$  kg. In the subsequent discussion, this result is first physically explained using Fig. 4d. Then a geometrical reason for the result shown in Fig. 4d is considered.

First, consider the reason why  $\theta_{\text{tilt}}$  is small for  $M_f \gg M_{fcr}$ , though the system contains massive propellant. This is because, for  $M_f \gg M_{fcr}$ , all values of  $z_{fGi}$  ( $i = 1-3$ ) are small, as shown in Fig. 4d. In the present example, the  $z$  coordinates of all of the components of the system, i.e., the main body of the satellite and objects 2 and 3 that have not yet been detached from the main body, are set to be 0 (such a case is common for a practical vehicle), so that the small values of  $z_{fGi}$  ( $i = 1-3$ ) yield small  $\theta_{\text{tilt}}$ .

Second, for very small  $M_f (\ll M_{fcr})$ ,  $\theta_{\text{tilt}}$  must be small, as shown by Fig. 4c, because the propellant is merely a negligible factor to cause a tilt of the principal inertia axis in spite of the large difference between  $z_{fG1}$  and  $z_{fG2} (= z_{fG3})$  found from Fig. 4d.

Third, for intermediate propellant mass, neither the propellant mass  $M_f$  nor the difference between  $z_{fG1}$  and  $z_{fG2} (= z_{fG3})$ , found from Fig. 4d, can be neglected. Thus, the tilt of the principal inertia axis is larger than for very large  $M_f$  and very small  $M_f$  and, consequently, must exhibit a maximum value. From the foregoing discussion, it can be concluded that the maximum of  $\theta_{\text{tilt}}$  is caused by the superpositional effect of the difference between  $z_{fG1}$  and  $z_{fG2} (= z_{fG3})$  (Fig. 4d) and the total propellant mass  $M_f$ .

Another important conclusion found is that the total propellant mass yielding the maximum tilt of the principal inertia axis is close to the critical total propellant mass  $M_{fcr}$ , under which one of the tanks gets empty.

Now, let us discuss the result shown in Fig. 4d. For the discussion, it is useful to divide the domain occupied by the liquid propellant in each tank into two parts: the spherical part and the conical part. These are given by the following.

Spherical part:

$$\tilde{x}_i^2 + \tilde{y}_i^2 + (\tilde{z}_i - b)^2 \leq a^2 \quad (i = 1, 2, 3) \quad (13)$$

Conical part:

$$\tilde{x}_i^2 + \tilde{y}_i^2 + (\tilde{z}_i - b)^2 \geq a^2 \quad (i = 1, 2, 3) \quad (14)$$

(cf. Fig. 1b). The spherical part is the domain whose distance from the center of the spherical surface of each teardrop tank is smaller than the radius  $a$ , whereas the conical part is the remaining domain. Let  $M_{fi\text{sph}}$  and  $M_{fi\text{coni}}$  denote the propellant masses in the spherical and the conical part of tank  $i$ , respectively. As  $M_{fi}$  (the propellant mass in the tank  $i$ ) increases,  $M_{fi\text{sph}}$  gets more and more predominant to  $M_{fi\text{coni}}$ . Irrespective of  $M_{fi}$ ,  $M_{fi\text{sph}}$  keeps its center of gravity in the plane  $z = 0$  when the liquid surface is cylindrical, as in the present case. Therefore, for large  $M_{fi}$ , each value of  $z_{fGi}$  ( $i = 1-3$ ) is close to 0, as shown in Fig. 4d. As  $M_{fi}$  becomes small, on the other hand, each  $z_{fGi}$  rises up, more and more sensitively depending on the decrease of  $M_{fi}$  because of the relative importance of  $M_{fi\text{coni}}$  toward  $M_{fi\text{sph}}$ . As a result, the values of  $z_{fG1}$  and  $z_{fG2} (= z_{fG3})$  exhibit the remarkable difference shown in Fig. 4d.

The discussions in the foregoing paragraph indicate that the presence of the conical part defined by Eq. (14) gives rise to different  $z_{fGi}$ , as mentioned earlier, and to the large maximum of  $\theta_{ilt}$  shown in Fig. 4c. If the conical part of each tank were neglected and each teardrop-shaped tank were approximated as a spherical tank, as in conventional studies, the difference between  $z_{fG1}$  and  $z_{fG2}$  ( $=z_{fG3}$ ) would vanish and all  $z_{fGi}$  ( $i = 1-3$ ) would be reduced to small values for all values of  $M_f$ , so that  $\theta_{ilt}$  would be underestimated. Therefore, so as to not underestimate  $\theta_{ilt}$ , it is essential to take the exact shape of the teardrop tanks into consideration. Such an exact treatment is a feature of present study.

#### Method for Reducing the Critical Propellant Mass and the Tilt of the Principal Inertia Axis

The fairly large critical propellant mass  $M_{fcr}$  shown in Fig. 4b (solid line for  $M_{f1}$ ) is a serious problem for an engine propulsion system because it causes suction of gas from the empty tank into the engine and, hence, much propellant mass ( $=M_{fcr}$ ) will be left unused. The large tilt of the principal inertia axis at the critical condition (Fig. 4c, solid line) also has an unfavorable influence on the attitude control of the spinning satellite. Therefore, we must consider a means to reduce  $M_{fcr}$  and  $\theta_{ilt}$ .

As explained in the preceding section, the large  $M_{fcr}$  is because of the remarkable difference between  $M_{f1}$  and  $M_{f2}$  ( $=M_{f3}$ ), whereas the large tilt of the principal inertia axis is because of the difference between  $z_{fG1}$  and  $z_{fG2}$  ( $=z_{fG3}$ ). Furthermore, the latter difference is caused by the former, as explained earlier in the discussion concerning Fig. 4d. Therefore, suppressing the difference between the propellant masses is useful for simultaneously reducing  $M_{fcr}$  and  $\theta_{ilt}$ . Such balancing between  $M_{f1}$  and  $M_{f2}$  ( $=M_{f3}$ ) can be accomplished by moving tank 1 outward, as shown in Fig. 2b, where the distance  $d_1$  between the  $z$  axis and the center of the spherical part of tank 1 is extended from 0.3 to 0.45 m after the detachment of object 1 by some mechanical apparatus for moving the tank. Here, note that the tank must be moved slowly to avoid sloshing. Such a device is perhaps useful because our main purpose is to accomplish the balance in stationary phase. The results for this new case are shown by dash-dot lines in Figs. 4a–4d for the sake of comparison with the earlier results (solid lines). Comparing the new and earlier results, one can confirm that in the new case both  $M_{fcr}$  and  $\theta_{ilt}$  are decreased. The value of  $M_{fcr}$  is seen to be reduced to 7 kg (Fig. 4b, dash-dotline for  $M_{f1}$ ). The value  $M_{fcr} = 7$  kg is much smaller than that for the earlier case ( $M_{fcr} = 37$  kg). It can also be ascertained by Fig. 4d that the difference between  $z_{fG1}$  and  $z_{fG2}$  (and, hence,  $z_{fG3}$ ) is reduced by the shift of tank 1.

In addition, one can see from Fig. 4a that the propellant migration restores the center of gravity less strongly than it did earlier. However, for the engine propulsion system and the attitude control system, restoring the center of gravity is less important than reducing  $M_{fcr}$  and  $\theta_{ilt}$ . Therefore, it is seen that an outward shift of the tank opposite to the detached object gives a real improvement.

#### Satellite-Liquid System with Objects 1 and 2 Detached

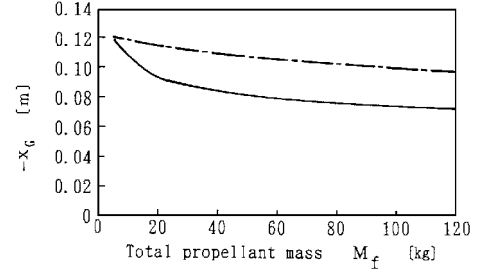
A numerical calculation is also performed for the case where objects 1 and 2 have been detached and object 3 is retained (Fig. 3). The results are shown in Figs. 5a–5d in a manner similar to Figs. 4a–4d. That is, the results shown by the dash-dot lines correspond to the case where the tanks 1 and 2 are moved farther from the  $z$  axis to reduce  $M_{fcr}$  and  $\theta_{ilt}$  simultaneously. The following similar tendencies can be reconfirmed.

1) The liquid propellant has an action of restoring  $G$  from  $x = -0.130$  m toward the  $z$  axis ( $x = 0$ ) to some degree (Fig. 5a). Here,  $x_G = -0.130$  m corresponds to the case  $M_f = 0$ , i.e., no propellant is contained in the system.

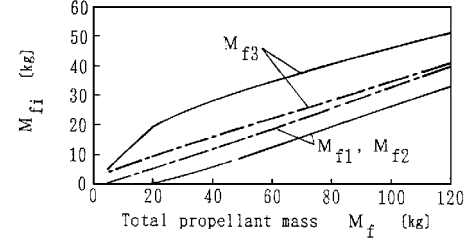
2) The slope  $|dx_G/dM_f|$  (solid line, Fig. 5a) is larger when tanks 1 and 2 are empty (for  $M_f$  smaller than the critical total propellant mass  $M_{fcr} = 20$  kg, Fig. 5b) than when no tank is empty.

3) From the comparison between the solid and dash-dot lines in Fig. 5a, the restoring action becomes weak due to the shift of tanks 1 and 2.

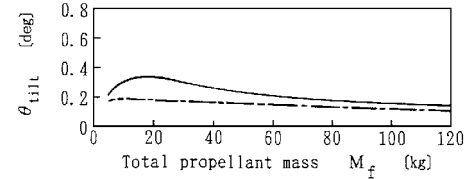
4) There exists a critical value of the total propellant mass  $M_{fcr}$ , for which tanks 1 and 2 near the center of gravity empty (Fig. 5b).



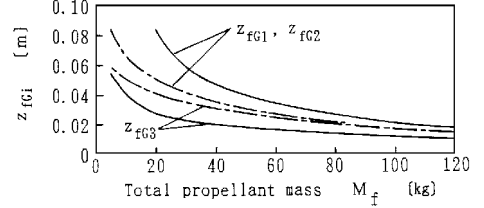
a)  $x$  coordinate  $x_G$  of the center of gravity for whole satellite-liquid system



b) Propellant masses  $M_{fi}$  in the tanks  $i$  ( $i = 1, 2, 3$ )



c) Tilt  $\theta_{ilt}$  of principal inertia axis vs  $\zeta$  axis



d)  $z$  coordinate  $z_{fGi}$  of the centers of gravity for liquid propellant in the tanks  $i$  ( $i = 1, 2, 3$ )

Fig. 5 Numerical results for the case where objects 1 and 2 are detached: —,  $d_1 = d_2 = d_3 = 0.3$  m and — — —,  $d_1 = d_2 = 0.45$  m;  $d_3 = 0.3$  m.

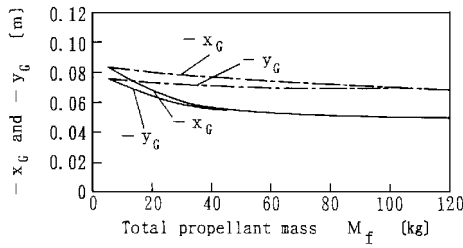
The value of  $M_{fcr}$  can be decreased by moving the tanks 1 and 2 farther away from the  $z$  axis.

5) The inclination  $\theta_{ilt}$  exhibits a maximum value near the critical propellant mass  $M_{fcr}$  (Fig. 5c).

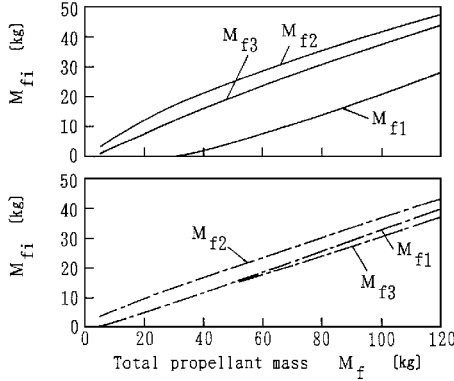
6) From comparison of the solid and dash-dot lines in Fig. 5c, one can see that  $\theta_{ilt}$  can be reduced by moving tanks 1 and 2 away from the  $z$  axis. This is because moving tanks 1 and 2 diminishes the difference between  $M_{f1}$  ( $=M_{f2}$ ) and  $M_{f3}$  and the difference between  $z_{fG1}$  ( $=z_{fG2}$ ) and  $z_{fG3}$ , as shown by Figs. 5b and 5d, respectively.

#### Asymmetric Case

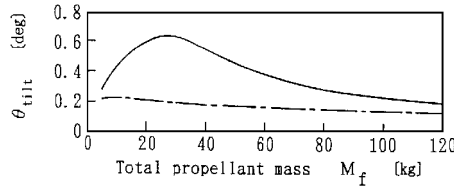
In these two examples, we have considered symmetric cases. The system is symmetric about the planes  $y = x/\sqrt{3}$  and  $y = -x/\sqrt{3}$ , respectively, for the cases shown in Figs. 4 and 5. Such symmetric cases are commendable for the sake of weight balancing. However, for practical applications there is the probable necessity of solving more difficult asymmetric problems. For an asymmetric case, we must find  $x_G$  and  $y_G$  independently. Typical results for an asymmetric case are shown in Fig. 6, where all parameters are exactly the same as earlier (Fig. 4), except that the mass of object 3 is decreased to 30 kg. From the comparison of the solid and dash-dot lines, it can be ascertained again that the movement of tank 1 is useful for reducing both the critical total propellant mass and the



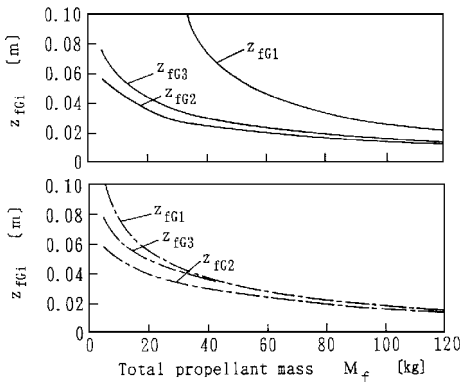
a) x coordinate  $x_G$  and y coordinate  $y_G$  of the center of gravity for whole satellite-liquid system



b) Propellant masses  $M_{fi}$  in the tanks  $i$  ( $i = 1, 2, 3$ )



c) Tilt  $\theta_{\text{tilt}}$  of principal inertia axis vs  $\zeta$  axis



d) z coordinate  $z_{fGi}$  of the centers of gravity for liquid propellant in the tanks  $i$  ( $i = 1, 2, 3$ )

Fig. 6 Asymmetric numerical example with object 1 detached: —,  $d_1 = d_2 = d_3 = 0.3$  m and ---,  $d_1 = 0.45$  m;  $d_2 = d_3 = 0.3$  m.

tilt of the principal inertia axis. It is noted that the circumferential coordinate of the center of the spherical part of tank 1 is shifted from 210 to 220 deg after the detachment of object 1 for coping with the asymmetry.

### Conclusions

The stationary position of the propellant in a teardrop tank system was determined for cases where fairly large displacements of the center of gravity are caused by the detachment of objects from the main body of a spinning satellite. The solution method and numerical results can be characterized as follows.

1) A double-loop iteration algorithm is applied to determine the unknown center of spin under the prescribed total propellant mass.

2) The teardrop shape of the tanks is taken into consideration exactly for accurately calculating mass, position of the center of

gravity, and inertia tensors of the propellant. Here, volume integration in spherical coordinates is found to be convenient.

3) Numerical results show that there exists a considerably large critical value of the total propellant mass below which some of the tanks become empty and that the tilt of the principal inertia axis becomes maximal at the critical condition.

4) The maximum of the tilt is caused by the presence of the conical parts of the teardrop tanks, so that the exact consideration of the teardrop shape of the tanks, which is the feature of the present study, is obligatory to avoid underrating the tilt of the principal inertia axis.

5) Critical total propellant mass and tilt of the principal inertia axis can be reduced simultaneously by moving some of the tanks outward in such a manner that the differences between the propellant masses of the tanks become small.

### Appendix: Evaluation of the Functions in Eqs. (9–12)

Compute  $\tilde{r}_i$  iteratively for an incrementing value of  $\tilde{z}_i$  according to the following equations, depending on  $\tilde{z}_i$ .

For  $0 \leq \tilde{z}_i \leq b - a \sin \theta_c$  (conical wall):

$$\tilde{r}_i = \tilde{z}_i \tan \theta_c \quad (\text{A1})$$

For  $b - a \sin \theta_c \leq \tilde{z}_i \leq b + a$  (spherical wall):

$$\tilde{r}_i = \{a^2 - (\tilde{z}_i - b)^2\}^{\frac{1}{2}} \quad (\text{A2})$$

and calculate  $\tilde{x}_i = \tilde{r}_i \cos \varphi_i$ ,  $\tilde{y}_i = \tilde{r}_i \sin \varphi_i$  for a fixed  $\varphi_i$  until the point  $(\tilde{x}_i, \tilde{y}_i, \tilde{z}_i)$  intersects the liquid surface expressed by Eq. (6). The angle  $\bar{\theta}_i(\varphi_i)$  then follows from

$$\bar{\theta}_i(\varphi_i) = \tan^{-1} \left( \frac{\tilde{r}_i}{a + b - \tilde{z}_i} \right) \quad (\text{A3})$$

When substituting Eq. (8) into Eq. (6), we can obtain an algebraic equation for  $R_i$ ,

$$a_i R_i^2 + b_i R_i + c_i = 0 \quad (\text{A4})$$

where  $a_i$ ,  $b_i$ , and  $c_i$  are functions of  $\theta_i$  and  $\varphi_i$ . The solution for  $R_i$  gives the function  $R_{iM}(\theta_i, \varphi_i)$ . The function  $R_{iW}(\theta_i, \varphi_i)$  can be determined by substituting Eq. (7) into Eqs. (A1) and (A2) and solving the resulting equation for  $R_i$ .

### Acknowledgments

The author is grateful to M. Kono and other members associated with the LUNAR-A project at the Institute of Space and Astronautical Science in Sagami-hara, Kanagawa Prefecture, Japan. The author wishes to thank Dirk Riechelmann of the Ishikawajima-Harima Heavy Industries Company, Ltd., for his work in the correction of the manuscript.

### References

- Ono, A., Nogawa, K., Iihara, S., Miyoshi, K., and Watanabe, T., "Development of Propulsion System for ISAS Lunar Exploration Project," *Ishikawajima-Harima Engineering Review*, Vol. 35, No. 2, 1995, pp. 77–82 (in Japanese).
- Honma, M., and Horikawa, Y., "Spin Axis Tilt of Satellite Induced by the Internal Fluid Migration," National Space Development Agency of Japan, TR-8, Tokyo, Japan, Jan. 1979.
- McIntyre, J. E., and Miyagi, M. I., "A General Stability Principle for Spinning Flexible Bodies with Application to the Propellant Migration-Wobble Amplification Effect," *ESA Symposium on Dynamics and Control of Non-Rigid Space Vehicles*, European Space Agency, Paris, 1976, pp. 159–175.
- Oberg, D. J., and Misra, P., "Propellant Management Operations on GSTAR-III," AIAA Paper 93-1800, June 1993.
- Ducret, E., Le Moullec, L., Spencer, B., and Balaam, P., "Propellant Management Device Studies, Computational Methods and Neutral Buoyancy Tests," AIAA Paper 92-3611, July 1992.
- Jaekle, D. E., Jr., "Propellant Management Device Conceptual Design and Analysis," AIAA Paper 93-1970, June 1993.
- Chapter, J. J., and Rider, S. B., "Surface Tension Propellant Management System Computerized Flow Analysis," AIAA Paper 80-1098, June–July 1980.